EUROfusion

EUROFUSION CP(15)05/63

C. Wersal et al.

The iInteraction Between Neutral Particles and Turbulent Plasma in the Tokamak SOL

(22nd June 2015 – 26th June 2015)
Lisbon, Portugal

This work has been carried out within the framework of the EUROfusion Consortium and has received funding from the Euratom research and training programme 2014-2018 under grant agreement No 633053. The views and opinions expressed herein do not necessarily reflect those of the European Commission.

The interaction between neutral particles and turbulent plasma in the tokamak SOL

C. Wersal, P. Ricci, F.D. Halpern, F. Riva

Ecole Polytechnique Fd́rale de Lausanne (EPFL), Centre de Recherches en Physique des Plasmas (CRPP), Lausanne, Switzerland

Abstract

The first-principle understanding of the processes in the Scrape-Off-Layer (SOL) of a tokamak is crucial for the development of a thermonuclear reactor. Since the plasma temperature in the SOL is rather low, the plasma is typically not fully ionized, and the neutral atoms play an important role in determining the SOL regimes. We have derived a kinetic model for neutral atoms in the SOL that contains the fundamental elements of neutral dynamics, while remaining relatively simple. The model has been coupled to the drift-reduced Braginskii equations and is implemented in GBS [1], a three-dimensional numerical code developed to simulate SOL turbulence. Details of the neutral model and the interactions with the plasma are given and we present first results indicating a transition into a regime that shows typical signatures of the conduction limited regime, e.g. significant parallel temperature gradients.

The neutral and plasma model

We describe the dynamics of the distribution function of a single mono-atomic neutral species, f_n, by using the following kinetic equation

$$\frac{\partial f_\mathrm{n}}{\partial t} + \vec{v}\cdot\frac{\partial f_\mathrm{n}}{\partial \vec{x}} = -\nu_\mathrm{iz} f_\mathrm{n} - \nu_\mathrm{cx}\left(f_\mathrm{n} - \frac{n_\mathrm{n}}{n_\mathrm{i}} f_\mathrm{i}\right) \tag{1}$$

being f_i, n_n, and n_i the ion distribution function, the neutral density, and the ion density, respectively. The ionization and charge-exchange processes are described, respectively, through the use of Krook operators with collision frequencies defined as $\nu_\mathrm{iz} = n_\mathrm{e}\langle v_\mathrm{e}\sigma_\mathrm{iz}(v_\mathrm{e})\rangle$ and $\nu_\mathrm{cx} = n_\mathrm{i}\langle v_\mathrm{i}\sigma_\mathrm{cx}(v_\mathrm{i})\rangle$, where $\langle\rangle$ is the average over the electron and ion distribution function, respectively. In the present work, the effective reaction rates, $\langle v\sigma\rangle$, are taken from the OpenADAS database (http://open.adas.ac.uk).

We consider a single ion species plasma. We start our derivation of the drift-reduced Braginskii equations from the kinetic Boltzmann equation of ions and electrons, where we include collision terms in the form of Krook operators to describe the interaction with the neutrals. The kinetic equation for the ions is

$$\frac{\partial f_\mathrm{i}}{\partial t} + \vec{v}\cdot\frac{\partial f_\mathrm{i}}{\partial \vec{x}} + \vec{a}\cdot\frac{\partial f_\mathrm{i}}{\partial \vec{v}} = \nu_\mathrm{iz} f_\mathrm{n} - \nu_\mathrm{cx}\left(\frac{n_\mathrm{n}}{n_\mathrm{i}} f_\mathrm{i} - f_\mathrm{n}\right) + C(f_\mathrm{i}) \tag{2}$$

while the kinetic equation for the electrons is

$$\frac{\partial f_\mathrm{e}}{\partial t}+\vec{v}\cdot\frac{\partial f_\mathrm{e}}{\partial \vec{x}}+\vec{a}\cdot\frac{\partial f_\mathrm{e}}{\partial \vec{v}}=\nu_\mathrm{iz}n_\mathrm{n}\left[2\Phi_\mathrm{e}(\vec{v}_\mathrm{n},T_\mathrm{e,iz})-\frac{f_\mathrm{e}}{n_\mathrm{e}}\right]+C(f_\mathrm{e}) \tag{3}$$

where $\vec{a}$ is the particle acceleration due to the Lorentz force, $\Phi_\mathrm{e}(\vec{v},T)$ is a Maxwellian distribution function for electrons, and $C(f_\mathrm{i})$ and $C(f_\mathrm{e})$ are the Coulomb collision operators. To derive the ionization operator in Eq. (3), we assume that a fast electron is lost, and two lower-energy electrons appear with a Maxwellian distribution function isotropically in the neutral frame of reference, and a temeprature, $T_\mathrm{e,iz}$, so that the total electron kinetic energy is reduced by the ionization energy, E_iz, giving $T_\mathrm{e,iz}=T_\mathrm{e}/2-E_\mathrm{iz}/3+m_\mathrm{e}v_\mathrm{e}^2/6-m_\mathrm{e}v_\mathrm{n}^2/3$, where T_e and v_e are the local electron temperature and fluid velocity respectively.

Following the work of Braginskii [3] and, e.g., Zeiler [4], we take the first three moments of the electron and ion kinetic equations in the limit $\omega_\mathrm{c}\tau\gg 1$, where $\omega_\mathrm{c}=qB/m$ is the gyrofrequency and τ the typical Coulomb collision time. Then, we simplify the hereby derived Braginskii equations in the drift limit, observing that $d/dt\ll\omega_\mathrm{ci}$ for typical SOL turbulence. The resulting drift-reduced Braginskii equations are

$$\frac{\partial n}{\partial t}=-\frac{1}{B}[\phi,n]+\frac{2}{eB}\left[C(p_\mathrm{e})-enC(\phi)\right]-\nabla_\parallel(nv_{\parallel\mathrm{e}})+\mathscr{D}_\mathrm{n}(n)+S_\mathrm{n}+n_\mathrm{n}\nu_\mathrm{iz} \tag{4a}$$

$$\frac{\partial\tilde{\omega}}{\partial t}=-\frac{1}{B}[\phi,\tilde{\omega}]-v_{\parallel\mathrm{i}}\nabla_\parallel\tilde{\omega}+\frac{m_\mathrm{i}\omega_\mathrm{ci}^2}{e^2n}\nabla_\parallel j_\parallel+\frac{2B}{cm_\mathrm{i}n}C(p)+\mathscr{D}_{\tilde{\omega}}(\tilde{\omega})-\frac{n_\mathrm{n}}{n}\nu_\mathrm{cx}\tilde{\omega} \tag{4b}$$

$$\begin{aligned}\frac{\partial v_{\parallel\mathrm{e}}}{\partial t}+\frac{e}{m_\mathrm{e}cn}\frac{\partial\Psi}{\partial t}=&-\frac{1}{B}[\phi,v_{\parallel\mathrm{e}}]-v_{\parallel\mathrm{e}}\nabla_\parallel v_{\parallel\mathrm{e}}+\frac{e}{\sigma_\parallel m_\mathrm{e}}j_\parallel+\frac{e}{m_\mathrm{e}}\nabla_\parallel\phi-\frac{T_\mathrm{e}}{m_\mathrm{e}n}\nabla_\parallel n\\&-\frac{1.71}{m_\mathrm{e}}\nabla_\parallel T_\mathrm{e}+\mathscr{D}_{v_{\parallel\mathrm{e}}}(v_{\parallel\mathrm{e}})+2\frac{n_\mathrm{n}}{n}\nu_\mathrm{iz}(v_{\parallel\mathrm{n}}-v_{\parallel\mathrm{e}})\end{aligned} \tag{4c}$$

$$\frac{\partial v_{\parallel\mathrm{i}}}{\partial t}=-\frac{1}{B}[\phi,v_{\parallel\mathrm{i}}]-v_{\parallel\mathrm{i}}\nabla_\parallel v_{\parallel\mathrm{i}}-\frac{1}{m_\mathrm{i}n}\nabla_\parallel p+\mathscr{D}_{v_{\parallel\mathrm{i}}}(v_{\parallel\mathrm{i}})+\frac{n_\mathrm{n}}{n}(\nu_\mathrm{iz}+\nu_\mathrm{cx})(v_{\parallel\mathrm{n}}-v_{\parallel\mathrm{i}}) \tag{4d}$$

$$\begin{aligned}\frac{\partial T_\mathrm{e}}{\partial t}=&-\frac{1}{B}[\phi,T_\mathrm{e}]-v_{\parallel\mathrm{e}}\nabla_\parallel T_\mathrm{e}+\frac{4T_\mathrm{e}}{3eB}\left[\frac{T_\mathrm{e}}{n}C(n)+\frac{7}{2}C(T_\mathrm{e})-eC(\phi)\right]+\frac{2T_\mathrm{e}}{3e}\left[\frac{0.71}{en}\nabla_\parallel j_\parallel-\nabla_\parallel v_{\parallel\mathrm{e}}\right]\\&+\mathscr{D}_{T_\mathrm{e}}(T_\mathrm{e})+\mathscr{D}_{T_\mathrm{e}}^\parallel(T_\mathrm{e})+S_{T_\mathrm{e}}+\frac{n_\mathrm{n}}{n}\nu_\mathrm{iz}\left[-\frac{2}{3}E_\mathrm{iz}-T_\mathrm{e}+m_\mathrm{e}v_{\parallel\mathrm{e}}\left(v_{\parallel\mathrm{e}}-\frac{4}{3}v_{\parallel\mathrm{n}}\right)\right]\end{aligned} \tag{4e}$$

$$\begin{aligned}\frac{\partial T_\mathrm{i}}{\partial t}=&-\frac{1}{B}[\phi,T_\mathrm{i}]-v_{\parallel\mathrm{i}}\nabla_\parallel T_\mathrm{i}+\frac{4T_\mathrm{i}}{3eB}\left[\frac{T_\mathrm{e}}{n}C(n)-\frac{10}{3}C(T_\mathrm{i})-eC(\phi)\right]+\frac{2T_\mathrm{i}}{3e}\left[(v_{\parallel\mathrm{i}}-v_{\parallel\mathrm{e}})\frac{\nabla_\parallel n}{n}-\nabla_\parallel v_{\parallel\mathrm{e}}\right]\\&+\mathscr{D}_{T_\mathrm{i}}(T_\mathrm{i})+\mathscr{D}_{T_\mathrm{i}}^\parallel(T_\mathrm{i})+S_{T_\mathrm{i}}+\frac{n_\mathrm{n}}{n}(\nu_\mathrm{iz}+\nu_\mathrm{cx})\left[T_\mathrm{n}-T_\mathrm{i}+\frac{1}{3}(v_{\parallel\mathrm{n}}-v_{\parallel\mathrm{i}})^2\right]\end{aligned} \tag{4f}$$

with $p=n(T_\mathrm{e}+T_\mathrm{i})$ the total pressure. The generalized vorticity, $\tilde{\omega}=\omega+1/e\nabla_\perp^2T_\mathrm{i}$, is related to the electrostatic potential by $\nabla_\perp^2\phi=\omega$, while $\nabla_\perp^2\Psi=j_\parallel$. The following operators have been introduced $\nabla_\parallel f=\mathbf{b}_0\cdot\nabla f$, $[A,B]=\hat{b}\cdot(\nabla A\times\nabla B)$, and $C(A)=\frac{B}{2}\left(\nabla\times\frac{\hat{b}}{B}\right)\cdot\nabla A$. The details of the model are presented in Ref. [2], where the boundary conditions and aditional collision processes are discussed.

Solution of the neutral kinetic equation in typical SOL relevant parameters

We now solve the kinetic advection equation for the neutrals, Eq. (1), by using the method of characteristics, under the assumption that plasma-related quantities are known. We consider two approximations, valid in the typical SOL parameter regime, which considerably simplify the solution, that is $\tau_{\text{neutral flight time}} < \tau_{\text{turbulence}}$ and $\lambda_{\text{neutral mean free path}} \ll 1/k_{\parallel,\text{plasma}}$, leading to a steady state solution of the neutral kinetic equation independently on each poloidal plane. Within these two approximations, the formal solution of the neutral kinetic equation, Eq. (1), is

$$f_\text{n}(\vec{x}_\perp,\vec{v}) = \int_0^{r_{\perp\text{b}}} \frac{\nu_\text{cx}(\vec{x}'_\perp) n_\text{n}(\vec{x}'_\perp)\Phi_\text{i}(\vec{x}'_\perp,\vec{v})}{v_\perp} \exp\left[-\frac{1}{v_\perp}\int_0^{r'_\perp} \nu_\text{cx}(\vec{x}''_\perp)+\nu_\text{iz}(\vec{x}''_\perp)dr''_\perp\right] dr'_\perp \qquad (5)$$

where $\vec{x}'_\perp = \vec{x} - r'_\perp \hat{\Omega}_\perp$ and $\hat{\Omega}_\perp = \vec{v}_\perp / v_\perp$. For better readability, we do not include the explicit notation of the t and $x_\parallel$ parametric dependencies. A linear integral equation for $n_\text{n}(\vec{x}_\perp)$ is obtained by integrating Eq. (5) in velocity space, which is

$$n_\text{n}(\vec{x}_\perp) = \int_D n_\text{n}(\vec{x}'_\perp)\nu_\text{cx}(\vec{x}'_\perp) K_{\text{p}\to\text{p}}(\vec{x}_\perp,\vec{x}'_\perp) dA', \qquad (6)$$

where we have rearranged the integrals, dA' is the infinitesimal area of D, which is the optically to $\vec{x}_\perp$ connected domain, and where the following kernel function has been defined

$$K_{\text{p}\to\text{p}}(\vec{x}_\perp,\vec{x}'_\perp) = \int_0^\infty \frac{1}{r'_\perp}\Phi_{\perp\text{i}}(\vec{x}'_\perp,\vec{v}_\perp) e^{-\frac{1}{v_\perp}\int_0^{r'_\perp}\nu_\text{eff}(\vec{x}''_\perp)dr''_\perp} dv_\perp, \qquad (7)$$

in which $\Phi_{\perp\text{i}}(\vec{x}_\perp,\vec{v}_\perp) = \int \Phi_\text{i}(\vec{x}_\perp,\vec{v}) dv_\parallel$. We remark that the kernel does neither depend on $f_\text{n}(\vec{x}_\perp,\vec{v})$, nor on any of its moments. After numerically solving Eq. (6), the distribution function of the neutral atoms, $f_\text{n}(\vec{x}_\perp,\vec{v})$, can be readily evaluated by using Eq. (5).

First plasma turbulence simulations with self-consistent neutral dynamics

The neutral model derived in this paper has been used to perform the first simulations of SOL plasma turbulence that include self-consistently the neutral dynamics. A newly developed version of the GBS code has been used for this purpose. We compare here a low plasma density simulation, $n_0 = 5\cdot 10^{18}\text{m}^{-3}$, with a high plasma density simulation, $n_0 = 5\cdot 10^{19}\text{m}^{-3}$. Both simulations consider a limited SOL geometry, with a toroidal limiter on the high field equatorial midplane, $R/\rho_{\text{s}0} = 500$, $m_\text{i}/m_\text{e} = 400$, $2\pi a = 800\rho_{\text{s}0}$, a being the minor radius, and $T_{\text{e}0} = 10\text{eV}$.

The poloidal dependence of the relevant plasma quantities for the low- and high-density simulations are shown in Fig. 1. The displayed profiles are averaged over a time window of 5 $R/c_{\text{s}0}$, over the full toroidal angle, and over a radial region extending for 20 $\rho_{\text{s}0}$, just outside the separatrix. We point out a few interesting differences between the high- and low-density simulations. The normalized density in the high-density simulation is flatter than in the low-density simulation. The plasma source due to ionization inside the SOL is much higher in the

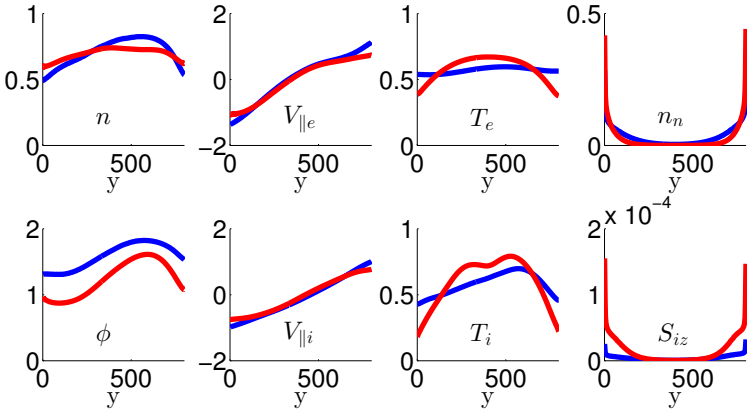

Figure 1: Time-averaged poloidal profiles of n, Φ, $V_{\|\mathrm{e}}$, $V_{\|\mathrm{i}}$, T_e, T_i, n_n, and S_iz for the low (blue) and high (red) plasma density scenario.

high-density simulation, so that there is a higher plasma source close to the limiter, preventing the plasma density to drop in this region. The parallel velocity profiles (which are expected to be approximately linear if the plasma source is poloidally constant) are somewhat flatter close to the limiters in the high-density scenario, however, the flattening is not particularly significant, because a relatively large fraction of the plasma density source is still due to the poloidally constant outflow of particles from the core. Both electron and ion parallel temperature gradients increase in the high-density scenario, which results in a higher amount of heat conduction as compared to the low-density simulation.

Acknowledgments

Part of the simulations presented herein were carried out using the HELIOS supercomputer system at Computational Simulation Centre of International Fusion Energy Research Centre (IFERC-CSC), Aomori, Japan, under the Broader Approach collaboration between Euratom and Japan, implemented by Fusion for Energy and JAEA; and part were carried out at the Swiss National Supercomputing Centre (CSCS) under Project ID s549. This work has been carried out within the framework of the EUROfusion Consortium and has received funding from the Euratom research and training programme 2014-2018 under grant agreement No 633053. The views and opinions expressed herein do not necessarily reflect those of the European Commission.

References

[1] P. Ricci, et al., Plasma Phys. Control. Fusion **54**, 124047 (2012)

[2] C. Wersal, et al., Submitted to Nuclear Fusion, May 2015

[3] S. I. Braginskii, Reviews of Plasma Physics **1** 205 (1965)

[4] A. Zeiler, et al., Phys. Plasmas, **4**(6) 2134 (1997)